

## Energy-loss distributions for 2.5-MeV He<sup>+</sup> ions incident on Si single crystals

M. A. Boshart, A. Dygo,\* and L. E. Seiberling

*Department of Physics, University of Florida, P.O. Box 118440, Gainesville, Florida 32611-8440*

(Received 17 October 1994)

The energy distributions for 2.5-MeV He<sup>+</sup> ions incident on thin Si single crystals are studied. Detailed angular scans are taken through the  $\langle 110 \rangle$  and  $\langle 100 \rangle$  axial directions along the  $\{111\}$  and  $\{110\}$  planar directions as well as perpendicular to the planar directions for Si(110) (0.74- and 1.4- $\mu\text{m}$ -thick) and Si(100) (0.75- $\mu\text{m}$ -thick) samples, respectively. Complex structures in the distributions are observed throughout the angular scans. The experimental distributions are reasonably well reproduced by a Monte Carlo simulation using the semiclassical approximation [N. M. Kabachnik, V. N. Kondratev, and O. V. Chumanova, *Phys. Status Solidi B* **145**, 103 (1988)] for energy loss to core electrons and the two-component free-electron-gas model for energy loss to valence electrons. Systematic deviations between theory and experiment are observed and discussed in terms of an increased penetration depth necessary for He<sup>+</sup> ions to become fully ionized when channeled.

PACS number(s): 61.80.Mk, 34.50.Bw, 79.20.Rf, 61.80.Jh

Investigations of energy-loss processes for ions interacting in single crystals have focused primarily on major axial and planar directions. This is due to a markedly reduced energy loss suffered by penetrating ions aligned with these high-symmetry directions over energy loss suffered when aligned with low symmetry ("random") directions [1]. The primary means of analysis of these early studies has been the peak or leading-edge value of the observed energy distributions [2]. This gives a narrow view of the impact-parameter dependence of the energy loss as essentially only impact parameters close to the channel radius are being explored.

A much better method is to model individual trajectories in the crystal by the Monte Carlo technique, attempting to fit the full experimental distributions, not just peak or leading edge values, allowing a study over a broader range of impact parameters. Furthermore, by tilting the crystal away from the axial (planar) direction, smaller impact parameters play an increasingly important role and complex structures can be obtained in the energy distributions [3]. The energy-loss model thus proposed should be valid for impact parameters that span the channel radius rather than just near the channel center.

Recently, we reported on the impact-parameter dependence of energy loss for 625-keV H<sup>+</sup> ions in Si single crystals [4]. Experimental energy distributions were obtained in the transmission geometry by scattering from a thin gold layer on the beam-exit side. Angular scans were taken through the  $\langle 110 \rangle$  and  $\langle 100 \rangle$  axial directions along the  $\{111\}$  and  $\{110\}$  planar directions as well as perpendicular to the planar directions for Si(110) and Si(100), respectively. The energy distributions were very well reproduced by the corresponding Monte Carlo simulation when the semiclassical approximation (SCA) of Kabachnik, Kondratev, and Chumanova [5] was used to describe the energy loss to core electrons and the free-

electron-gas (FEG) model was used to determine the valence-electron contribution to the stopping.

Adhering very closely to this outline, in this Brief Report the energy-loss distributions for 2.5-MeV He<sup>+</sup> ions (velocity unchanged from 625-keV protons) incident on silicon single crystals are studied as a function of crystal orientation. However, the above model is a first-order perturbation calculation for a bare nucleus and our incident beam is He<sup>+</sup>. Deviations may be expected if the He<sup>+</sup> ions do not become fully ionized near the surface. Incident He<sup>2+</sup> would perhaps be better suited to our energy-loss model, but He<sup>+</sup> beams are readily available and thus widely used in energy-loss studies [6–11] and analytical applications [12].

As the experimental procedure is similar to that described in Ref. [4], the principal points of the procedure are given here along with any differences from the previous experiment. The incident beam of 2.5-MeV He<sup>+</sup> ions was produced by the University of Florida 3.5-MV Van de Graaff accelerator and collimated to a cross-sectional area of  $0.8 \times 0.8 \text{ mm}^2$  and an angular divergence of  $0.03^\circ$ . Three samples, 0.74- $\mu\text{m}$ -thick Si(110), 1.4- $\mu\text{m}$ -thick Si(110), and 0.75- $\mu\text{m}$ -thick Si(100), were prepared using a dopant-selective etching technique [13] and a 10- $\text{\AA}$ -thick amorphous layer of Au was deposited onto the 10% HF-dipped surface. The samples were mounted on a two-axis goniometer, stepper motor driven with a resolution of  $0.02^\circ$ . The ions scattered through  $65^\circ$  were detected in a transmission geometry (the Au layer on the beam-exit side, as shown in Fig. 1) and energy analyzed using a Si surface-barrier detector with an acceptance angle of  $2.5^\circ$ . The scattering yield from Si was used to align planar and axial directions to the beam. The alignment for any direction in the crystal was achieved to a precision of  $0.02^\circ$ – $0.05^\circ$ . Finally, the energy distributions of the He ions transmitted through the Si single crystal were retrieved from the Au signal by dividing the measured energy by the kinematic factor.

For each set of angular scans, a total of 22 distributions were taken on the same target spot to ensure no variation in sample thickness. Each distribution was col-

\*On leave from the Soltan Institute for Nuclear Studies, Warsaw, Poland.

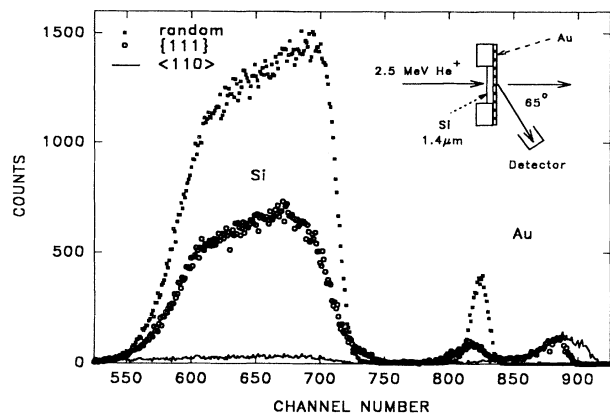


FIG. 1. Energy spectra for 2.5-MeV He ions transmitted through 1.4- $\mu\text{m}$ -thick Si crystal and scattered through 65°, taken in the random directions, aligned with the  $\{111\}$  planar and aligned with the  $\langle 110 \rangle$  axial directions.

lected for 0.8  $\mu\text{C}$  of the integrated beam charge. Two angular scans were performed: (1) through the  $\langle 110 \rangle$  and  $\langle 100 \rangle$  axial directions along the  $\{111\}$  and  $\{110\}$  planar directions and (2) perpendicular to the  $\{111\}$  and  $\{110\}$  planes at tilt  $\theta=10^\circ$  and  $4^\circ$  with respect to the  $\langle 110 \rangle$  and  $\langle 100 \rangle$  axes for Si(110) and Si(100), respectively. The directions  $(\theta, \phi)=(10^\circ, 10^\circ)$  and  $(\theta, \phi)=(4^\circ, 12^\circ)$  were taken as an approximation to random incidence for Si(110) and Si(100), respectively [4,14].

Additionally, a number of randomlike spectra were also taken to monitor and correct for carbon deposition during the irradiation [about  $10^{16}$  C atoms/( $\text{cm}^2\mu\text{C}$ ) deposited on both sides]. A repeated measurement of the axial direction at the end of the experiment was used to check for structural damage due to the irradiation (found to be negligible). Finally, the sample thickness, the normalization constant for all distributions, as well as the overall energy resolution were determined based on the distribution for the random direction (see above) by requiring that the simulated distribution matched the experiment. The overall energy resolution was found to be from about 15 to 25 keV (experiment dependent). This value includes the detection system resolution, the energy spread of the incident beam, and the effect of the sample nonuniformity.

The CXX simulation code [14,15] has been used to calculate channeled ion trajectories and their energy distributions. The simulations made use of the He-Si interaction potential based on the Hartree-Fock electronic density modified for solid-state effects [16]. The silicon vibrational amplitude of 0.078 Å was considered in three dimensions and a beam divergence of 0.03° was included. A simulated distribution was generated by following 3200–6400 trajectories at a given  $(\theta, \phi)$  [taking roughly 2 h computing time on a personal computer (Intel 486DX-33)]. Energy straggling, calculated based on Ref. [17], and the energy dependence of the He-Au cross section were taken into account separately.

In order to calculate the energy loss, the simulation employs the model found to yield the best fits to the data

in our study of 625-keV  $\text{H}^+$  ions incident on silicon. A detailed description of that model can be found in Ref. [4]. We highlight key points here.

We make the usual assumption that core and valence electrons contribute independently to the stopping. For core electrons, the impact-parameter-dependent stopping is calculated within first-order perturbation theory using the SCA model [5]. The method involves an explicit summation of all contributions due to excitation and ionization of the atom, which is described by the Hartree-Slater approximation.

The interaction of the ion with valence electrons is treated within FEG theory. The energy losses are divided into a contribution due to single-particle excitations that occur in close collisions with valence electrons and a contribution due to collective excitations. The first contribution is taken to be proportional to the local valence electron density, while the latter contribution is proportional to the average electron density. Utilizing the x-ray-diffraction measurements of Deutsch [18], two-dimensional maps of electron density (integrated along the ion's trajectory) across the  $\langle 110 \rangle$  and  $\langle 100 \rangle$  channels were calculated and used in the simulations to calculate the stopping in close collisions with valence electrons.

The above model is easily adapted from 625-keV H ions to 2.5-MeV He ions by setting  $Z_1^2=4$ , as the velocity is unchanged. Further, we require that the integral over all impact parameters reproduce the stopping cross section given in Ref. [19]. Based on our previous work [4], it was found that reducing the cross section of both components of valence stopping by 6% from the value given by the two-component FEG theory gave the best fits to the data. Therefore, the core electron stopping cross section had to be raised by 12% from the SCA calculation.

The simulation results for a set of 12 representative distributions are compared with the experimental data in Figs. 2–4. Figure 2 is for a 0.74- $\mu\text{m}$  Si(110) sample, Fig. 3 is for a 1.4- $\mu\text{m}$  Si(110) sample, and Fig. 4 is for a 0.75- $\mu\text{m}$  Si(100) sample. It is evident from the comparisons that the data can be reasonably well reproduced using the energy-loss model discussed. It is also clear from the data that systematic deviations between experiment and theory exist that were not present in the  $\text{H}^+$  incident ion case [4]. The deviations between theory and experiment in all data sets are pronounced on the high-energy side of the energy distributions, where the simulated distributions are shifted to lower energies with respect to the data. Further, scans near the  $\langle 100 \rangle$  axis (Fig. 4) match the theory better than either scans near the  $\langle 110 \rangle$  axis (Figs. 2 and 3) and scans performed on the 1.4- $\mu\text{m}$  Si(110) sample are predicted by the theory better than scans on the thinner 0.74- $\mu\text{m}$  Si(110) sample. Finally, one notices that the point  $(\theta, \phi)=(0.2, 0)$  is reproduced by the theory surprisingly well in Figs. 2 and 3, even though it is surrounded by points exhibiting marked deviations. We will try to address these issues.

The first point that must be made concerns the fact that the incident beam in the experiments was  $\text{He}^+$  rather than  $\text{He}^{2+}$ , while the energy-loss model employed assumes a bare nucleus ( $\text{He}^{2+}$  ion) within the silicon crys-

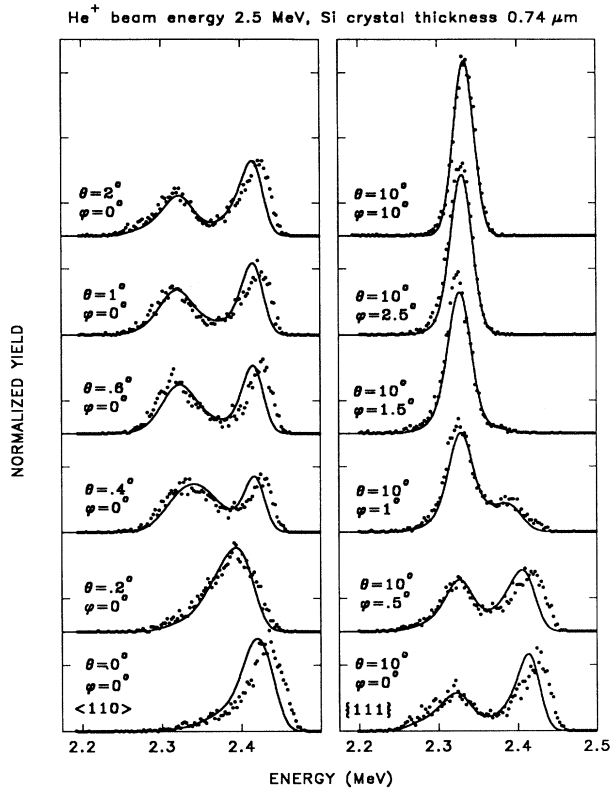


FIG. 2. Monte Carlo simulated energy distributions (solid lines) using the energy-loss model described in the text compared with experimental data (dots) for directions near the  $\langle 110 \rangle$  axis (Si crystal thickness 0.74  $\mu\text{m}$ ).

tal. In random incidence or amorphous targets, one may assume that after some "short" (5 Å in silicon [20]) distance within the crystal, virtually all 2.5-MeV He<sup>+</sup> ions (more than 95%) are stripped and become He<sup>2+</sup> ions, making the energy-loss model fully applicable. The channeling effect, however, steers many ions "far" (1–2 Å) away from the host atoms, keeping them in a reduced electron density, and the tendency to lose a second electron is reduced. Therefore, an important difference from the H<sup>+</sup> ion experiment is introduced: well-channeled partially stripped He<sup>+</sup> ions may survive to large penetration depths.

The disagreement between theory and experiment can be explained in terms of the above supposition in that well-channeled He<sup>+</sup> ions would suffer substantially reduced stopping compared to the assumed model [21]. This would shift the high-energy side of the simulated distributions to lower energy as compared to the data, since the high-energy side corresponds to well-channeled particles and the simulation assumes the enhanced stopping of a bare nucleus for all ions. The low-energy side of the simulated distributions would be expected to agree with the measured distributions since ions moving close to atomic strings will be completely ionized much more quickly. In this way, the overall deviation between experiment and theory can be qualitatively explained by the He<sup>+</sup> incident beam. This explanation seems to be at vari-

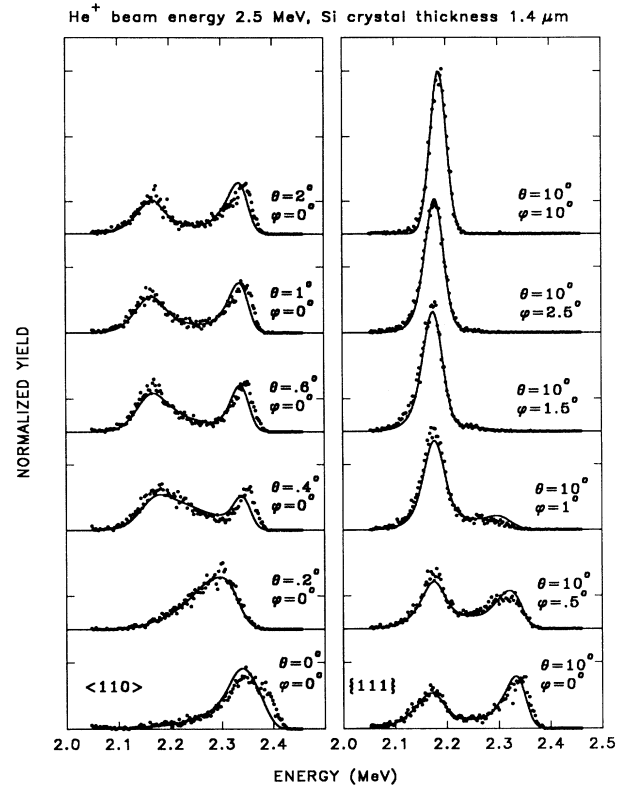


FIG. 3. Same as Fig. 2, but for 1.4- $\mu\text{m}$ -thick Si.

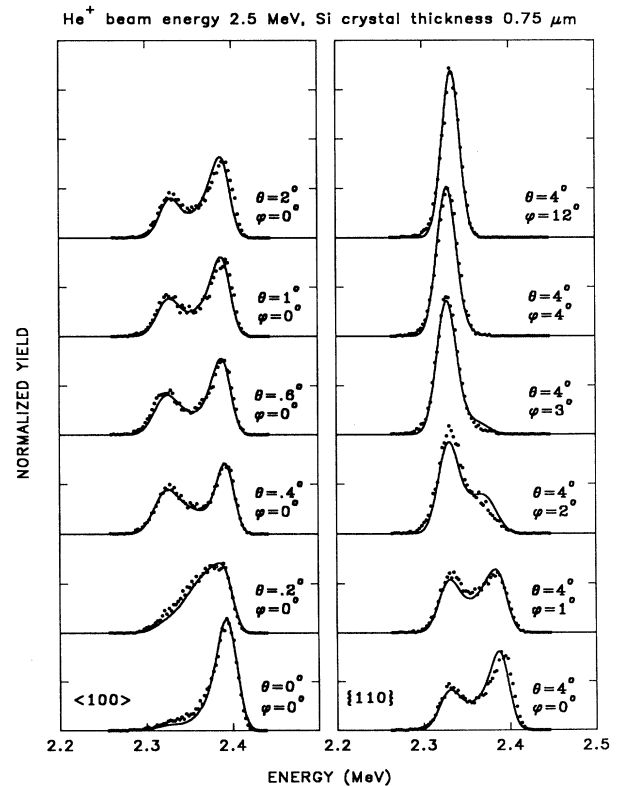


FIG. 4. Same as Fig. 2, but for directions near the  $\langle 100 \rangle$  axis and 0.75- $\mu\text{m}$ -thick Si.

ance with the conclusions concerning the survival rate of 2-MeV  $\text{He}^+$  ions in GaAs:Er, found in Ref. [11].

In considering the differences in the deviation between the data sets, since the  $\langle 100 \rangle$  channel has a smaller radius than the  $\langle 110 \rangle$  channel (1.36 Å compared to 2.04 Å) and a larger electron density in the middle of the channel as a result [4], one might expect even well-channeled  $\text{He}^+$  incident ions to be fully stripped near the surface. This would explain the better agreement between theory and experiment in the  $\langle 100 \rangle$  experiment than either  $\langle 110 \rangle$  experiment. In addition, the 1.4- $\mu\text{m}$  Si(110) scans agree better with the theory than the 0.74- $\mu\text{m}$  Si(110) scans and this may be due to the fact that the ions spend more time completely stripped penetrating the thicker crystal. The absolute (dis)agreement with experiment should be roughly the same then, but the relative (dis)agreement is much improved in the thicker sample's scans as the partially stripped ions survive for some penetration depth which is a smaller fraction of the total distance traveled in the thicker sample (the shift between simulation and experiment for the axial direction is 16 keV for Fig. 2 and 19 keV for Fig. 3).

A final point concerns that apparent anomalous agreement between the simulation and experiment for the point  $(\theta, \phi) = (0.2, 0)$  in Figs. 2 and 3, even though surrounding data points display deviations. This can be explained in terms of the axial to planar channeling transition. As shown in Ref. [4], there is a region in the axial to planar channeling transition where axial channeling is

suppressed due to the tilt from the axis, but planar channeling has not yet manifested itself. Therefore, there is simply no sizable well-channeled component of the beam at this point and the  $\text{He}^+$  ions become fully stripped near the surface.

In conclusion, the comparison between experimental and Monte Carlo simulated energy distributions shows that a first-order perturbation calculation of energy loss (the SCA model for core electron stopping and the two-component FEG model for valence electron stopping) describes reasonably well the stopping of 2.5-MeV  $\text{He}^+$  ions incident on thin silicon single crystals. This model reproduces the data throughout detailed angular scans around major axes in silicon, showing its validity over a wide range of impact parameters. However, systematic deviations are observed for directions close to the  $\langle 110 \rangle$  axis in silicon. These deviations can be explained if well-channeled  $\text{He}^+$  incident ions are penetrating deep into the crystal before becoming fully stripped, suffering reduced stopping compared to the theory.

We are grateful to N. M. Kabachnik for valuable discussions and providing us with the results of his SCA calculations. We would also like to gratefully acknowledge the technical assistance of R. Johns. This work was supported by the NSF (Grant No. DMR-9413245) and the University of Florida Division of Sponsored Research and the College of Liberal Arts and Sciences.

- 
- [1] D. S. Gemmell, *Rev. Mod. Phys.* **46**, 129 (1974).  
 [2] M. A. Kumakhov and F. F. Komarov, *Energy Loss and Ion Ranges in Solids* (Gordon and Breach, New York, 1981), and references therein.  
 [3] A. Dygo, M. A. Boshart, M. W. Grant, and L. E. Seiberling, *Nucl. Instrum. Methods B* **93**, 117 (1994).  
 [4] A. Dygo, M. A. Boshart, L. E. Seiberling, and N. M. Kabachnik, *Phys. Rev. A* **50**, 4979 (1994).  
 [5] N. M. Kabachnik, V. N. Kondratev, and O. V. Chumanova, *Phys. Status Solidi B* **145**, 103 (1988).  
 [6] R. J. Culbertson, S. P. Withrow, and J. H. Barrett, *Nucl. Instrum. Methods B* **2**, 19 (1984).  
 [7] H. S. Jin and W. M. Gibson, *Nucl. Instrum. Methods B* **13**, 76 (1986).  
 [8] P. F. A. Alkemade, W. C. Turkenburg, and W. F. van der Weg, *Nucl. Instrum. Methods B* **28**, 161 (1987).  
 [9] K. Kimura, M. Hasegawa, and M. Mannami, *Phys. Rev. B* **36**, 7 (1987).  
 [10] K. Narumi *et al.*, *J. Phys. Soc. Jpn.* **62**, 1603 (1993).  
 [11] Y. Kido *et al.*, *Phys. Rev. B* **49**, 14 387 (1994).  
 [12] W. K. Chu, J. W. Mayer, and M. A. Nicolet, *Backscattering Spectrometry* (Academic, Orlando, 1978).  
 [13] L. E. Seiberling, P. F. Lyman, and M. W. Grant, *J. Vac. Sci. Technol. A* **11**, 715 (1993).  
 [14] A. Dygo, W. N. Lennard, I. V. Mitchell, and P. J. M. Smulders, *Nucl. Instrum. Methods B* **84**, 23 (1994); **90**, 161 (1994).  
 [15] A. Dygo and A. Turos, *Phys. Lett. A* **127**, 281 (1988); *Phys. Rev. B* **40**, 7704 (1989).  
 [16] A. Dygo, P. J. M. Smulders, and D. O. Boerma, *Nucl. Instrum. Methods B* **64**, 701 (1992); **67**, 185 (1992).  
 [17] Q. Yang and D. J. O'Connor, *Nucl. Instrum. Methods B* **61**, 149 (1991).  
 [18] M. Deutsch, *Phys. Rev. B* **45**, 646 (1992).  
 [19] J. F. Ziegler, *Helium: Stopping Powers and Ranges in All Elemental Matter* (Pergamon, New York, 1977).  
 [20] J. C. Armstrong, J. V. Mullendore, W. R. Harris, and J. B. Marion, *Proc. Phys. Soc. (London)* **86**, 1283 (1965).  
 [21] L. R. Logan, C. S. Murthy, and G. R. Srinivasan, *Phys. Rev. A* **46**, 5754 (1992).